PERGAMON

International Journal of Heat and Mass Transfer 42 (1999) 599–612

International Journal of HEAT and MASS TRANSFER

Heat transfer in a wall jet at high turbulence of cocurrent stream

V. P. Lebedev*, V. V. Lemanov, V. I. Terekhov

S. S. Kutateladze's Institute of Thermophysics, Siberian Division of the Russian Academy of Sciences, 630090, Novosibirsk, Russia

Received 23 June 1998

Abstract

Heat transfer is studied at an extending of a wall jet in a cocurrent stream in wide variation range of injection parameter ($m < 1$ and $m > 1$) and turbulence level of the stream ($Tu_0 = 0.2$–20%). A rise in turbulence at $m < 1$ is shown to increase heat transfer by 20%, and both the adiabatic wall temperature and relative heat-transfer function should be taken into account when calculating heat transfer. In the $m > 1$ regime, turbulence level has no effect on heat transfer, so that the latter can be estimated according to relationships being valid for low-turbulent jet flows.

Nomenclature

c_p specific heat capacity
E_u spectrum of longitudinal velocity pulsations
f frequency
K_j dimensionless parameter $(x-x_1)(sRe_s^{0.25})$
l_u longitudinal integral turbulence scale
m injection parameter, $\rho_s U_s/\rho_0 U_0$
n exponent in the power velocity profile
Pr Prandtl number, $\mu c_p/\lambda$
q heat flux
Re Reynolds number, $Re_0 = \rho_0 U_0 D/\mu_0$, $Re_s = \rho_s U_s s/\mu_s$, $Re_T^{**} = \rho_0 U_0 \delta_T^{**}/\mu_0$
St Stanton number
s slot height
T temperature
Tu turbulence level
U velocity
x longitudinal coordinate
x_1 starting heated length of the wall jet
y transverse coordinate.

Greek symbols

α heat-transfer coefficient
$\delta,\delta^*,\delta^{**}$ boundary layer, displacement and momentum thickness
δ_T^{**} energy thickness
ε turbulent energy dissipation rate
η dimensionless coordinate, $\rho U* y/\mu$
Π velocity profile parameter
Θ gas screen cooling effectiveness $(T_{wa}-T_0)/(T_s-T_0)$
κ wave number
μ dynamic velocity
ρ density
φ dimensionless velocity, $U/U*$
ψ relative heat-transfer function at $Re_T^{**} = \text{idem}$, St/St_0.

Subscripts

a adiabatic conditions
s secondary stream
w at wall
0 main stream, standard conditions.

1. Introduction

Wall jets are widely used in up-to-date apparatuses and technologies. One of the problems of current interest in using them is estimation of heat exchange between a gas stream and a channel wall aimed at determination of highest permissible surface temperatures and heat fluxes. The heat transfer in real apparatuses is often realized at high intensity of pulsational velocity. For example, in combustion chambers of gas-turbine and rocket engines the turbulence level may run into 30–40%.

* Corresponding author

S0017–9310/98 $19.00
PII: S0017–9310(98)00180–X

Eckert [1] has proposed to calculate the local heat-transfer coefficient at gas injection into boundary layer according to the following expression:

$$\alpha = \frac{q_w}{T_w - T_{wa}} \tag{1}$$

where T_{wa} is the wall temperature under adiabatic conditions. In [2], it has been shown that the integral relationship for energy in a boundary layer with gas blowing retains the same form as in the case without it provided that the thermal energy thickness and the Stanton number are determined as

$$\delta_T^{**} = \int_0^\infty \frac{\rho U}{\rho_0 U_0} \frac{T - T_a}{T_w - T_{wa}} dy,$$

$$St = \frac{q_w}{\rho_0 c_{p0} U_0 (T_w - T_{wa})}. \tag{2}$$

Here T and T_a are the temperatures at the point of interest in the boundary layer on the heat exchanging surface and on the adiabatic one.

When calculating convective heat transfer, the power law [3]

$$St = \frac{B/2}{(Re_T^{**})^m Pr^k}, \tag{3}$$

if widely used, the coefficients B and m entering it being dependent upon the power exponent n in the power velocity profile

$$\frac{U}{U_m} = A(n) \left(\frac{y}{\delta^{**}}\right)^{1/n}. \tag{4}$$

In [4], it has been shown experimentally that under conditions of a film cooling the temperature profiles in boundary layer plotted with due regard to T_{wa} are similar to velocity profiles and they can be generalized with the power dependence (4). The heat transfer law has the form (3) and for the 'standard' boundary layer (a gradientless incompressible isothermal flow with a low-intensity turbulence, $1/n = 1/7$), in view of (2), it can be written as

$$St_0 = \frac{0.0128}{(Re_T^{**})^{0.25} Pr^{0.75}}. \tag{5}$$

The heat transfer at blowing gas into boundary layer has been extensively studied for the low-turbulent stream [3; 5–8] when the turbulence level does not exceed 4–5%. In a number of works [9–12], the effect of slot turbulence on the spreading of wall jets was studied. It has been established that turbulence only has a pronounced effect on the jet within the starting length. A study of heat transfer in a wall jet at an increased free-stream turbulence ($Tu_0 = 9.3\%$) has been reported in [13]. A considerable effect of external turbulence on the starting jet length has been found. Upon increasing turbulence level from 1.7% up to 9.3%, the heat-transfer coefficient was found to change: (a) by 3–8% in case of perforated blowing, (b) by 7–13% and 20–70% for gas injection through a slot of height $s = 1$ mm and 3.8 mm, respectively. As the main stream, the starting length of a submerged jet was used, the heat-transfer coefficient being determined for the temperature of injected gas being equal to that of the main stream.

In [14], the effect of turbulence on heat transfer under conditions of slot film cooling was determined through calculations. At the maximum turbulence of 20% used, the increase in heat transfer amounted to 70–100% for the velocity ratio $U_s/U_0 = 0.5$ and for $T_s/T_0 = 0.3$, which is indicative of a considerable influence of flow turbulence on heat transfer. According to [15–18], the highest effect of the intensity of external turbulence on heat transfer in the case without injection is up to 50%.

In [19], the external turbulence was experimentally shown to increase the heat-transfer coefficient in the screen zone (blowing through a porous section). The external turbulence shifts the point where the boundary layer gets detached from the wall and intensifies wall mass-transfer, interfering with the formation of a recirculation flow in the front part of the screen zone. The data on heat transfer in the screen zone at high turbulence ($Tu_0 = 13$–17%) can be generalized by the dependence (3) with the power exponent $1/n = 1/6$ and high blowing parameters. The authors have pointed to a noticeable influence on heat transfer of dynamic pre-history and injection parameter.

The data on heat transfer reported in [13] have been obtained for $T_s = T_0$, while in [14] Stanton number was determined from the difference between the wall and stream temperatures. In [19], the heat transfer law was found to depend upon the value of blowing ratio through porous wall. Experimental data on heat transfer in the slot-screen zone upon varying the approach-stream intensity are lacking. When calculating film cooling, one should know if the heat transfer law (5) remains conservative under the action of increased turbulence at slot gas injection, and additional experimental data are needed to clear up this question.

2. Experimental equipment

The scheme of the working section is shown in Fig. 1. The tests were carried out in a cylindrical channel 6 (diameter $D = 80$ mm, length $L = 250$ mm, wall thickness 2 mm). The wall jet was formed by blowing air from an injection chamber 4 through a tangential annular slot of height $s = 2$ mm. The separator 3 and the fairing 5 are made of caprolan and textolite, respectively. The turbulence generator 1 was installed inside the prechamber of the wind tunnel in front of the converging tube 2 with the contraction ratio 6.9. The distance between the turbulence generator 1 to the slot was 264 mm. The turbulence generator 1 represented a steel 4 mm-thick

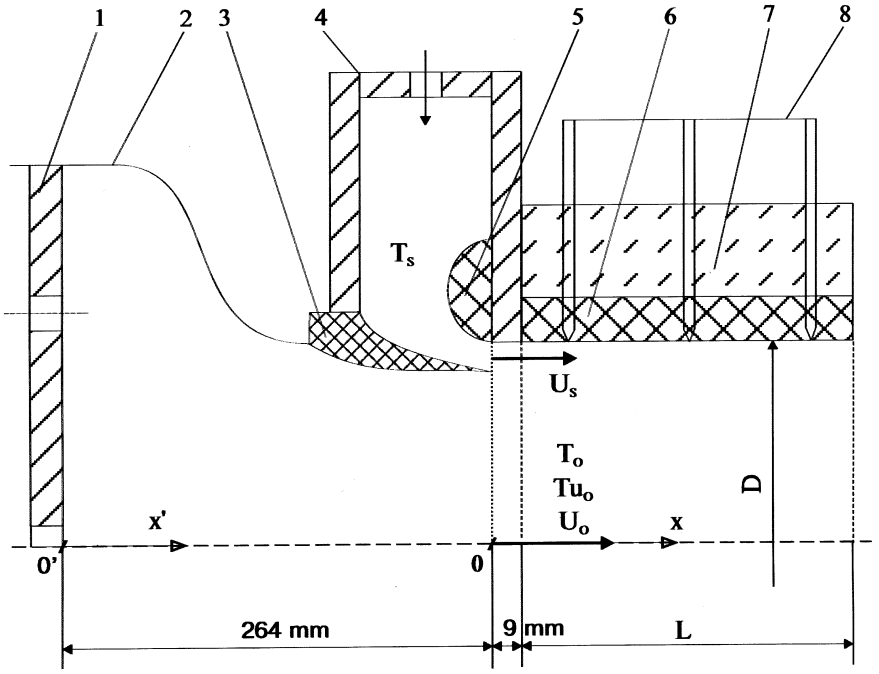

Fig. 1. Scheme of the experiment: (1) turbulence generator, (2), converging tube, (3) separator, (4) injection chamber, (5) fairing, (6) working channel, (7) thermal insulator, (8) thermocouples.

plate with 4, 7, 13, or 25 holes of 14 mm diameter (the geometry is described in [20, 21]. Upon substituting a fine-mesh net (S-1) instead of the plate, the turbulence level of 0.2% could be realized. Such a layout of turbulence generators provided at the inlet of the working section: (a) uniform profiles of mean and pulsational velocities (the flatness of mean velocity—2–5%, that of pulsational components—6–10%, (b) high (up to 15–20%) intensity of isotropic turbulence.

In heat-transfer studies, the condition $q_w = \text{const}$ was fulfilled, the heat flux (with the maximum value up to 5000 W/m^2) being generated by ohmically heating the channel wall. The working channel 6 was made of stainless steel and covered with a heat-insulating layer 7. In order to diminish longitudinal heat overflows, circular grooves of 1 mm depth were made at a few cross-sections over the length of the cylinder. Thermal measurements were carried out with chrome-copel thermocouples 8 made of wire of 0.2 mm-diameter. Thermo-emf was measured with an F30 voltmeter with an accuracy of 0.1%. The inaccuracy in determining temperature over the 15–100°C range was 0.15°C. The power generated by the electric heater was measured by a D57 wattmeter with the accuracy rating 0.1. The heat losses caused by emitting radiation and by heat conductivity through the thermoinsulator and through the edge surface of the channel did not exceed 4–6%. When determining St, the allowance for the effect of non-isothermality was made according to [3]. The estimated rms value of the inaccuracy in the measured heat-transfer coefficient was 5–7%, while that in Stanton number 6–8%.

Turbulent characteristics were measured using an automated complex based on a DISA 55M constant-temperature hot-wire anemometer [22]. The estimated rms value of the inaccuracy in the turbulence level (the estimation was made in [22]) over the range $Tu = 0.2$–20% was 5–12%, the highest among different components being the inaccuracies caused by instability of the calibration characteristic of the probe, high level of turbulence and measuring facilities.

Parameters of the main stream in the experiment were: velocity $U_0 = 15$ m s^{-1}, Reynolds number $Re_0 = 8 \times 10^4$, temperature $T_0 \approx 300$ K, turbulence level $Tu_0 = 0.2$–20%. Parameters of the wall jet were: velocity $U_s = 3$–30 m s^{-1}, Reynolds number $Re_s = 700$–6700, temperature $T_s \approx 363$ K, turbulence level $Tu_s = 5$–7%. The injection parameter m amounted to 0.2–0.5.

2.1. Physical modelling of turbulent streams

Modelling of turbulence in laboratory setups faces some difficulties. The latter is caused by the fact that the turbulent stream possesses a number of parameters characterizing its statistical nature such as turbulent energy, turbulence level, scale characteristics, spectral and correlative functions, rate of dissipation etc. Nor-

mally the modelling boils down to fulfilling equality between turbulence levels under laboratory and full-scale conditions, and only in some works comparison between longitudinal integral turbulence scales was made. In opinion of the authors of [16, 17], the involvement of a multitude of parameters is a main reason of the existing discrepancy between experimental data which is revealed upon comparing them. In this connection, considerable attention in this work is paid to modelling turbulence parameters and fixing initial conditions in the problem on studying the extending wall jet in a cocurrent high-turbulent stream.

Figure 2 presents experimental data on the turbulence level at the channel axis in the exit section of slot as dependent upon the flow-core velocity. The experiments are presented which were carried out using three turbulence generators PP-7, PP-13, PP-25 and an S-1 net. As seen from the figure, using the turbulence generators and the net has allowed to cover the range of the intensity of pulsations from 0.2% up to 15%. The level of turbulent fluctuations weakly depends upon the stream velocity and at a fixed distance downstream from the turbulence generator it can be represented in the form [16]:

$$Tu^2 = \frac{c}{U^m}. \tag{6}$$

The constant c and the power exponent m are given in Table 1. Under the conditions of the experiments ($Re_0 = 8 \times 10^4$), the turbulence at the slot exit section was: behind the S-1 net—0.2%, behind the turbulence generators PP-25, PP-13, PP-7 and PP-4—from 7%, from 12%, from 15% and 20%, respectively. The anisotropy of the components of pulsational velocity did not exceed: for the PP-4 turbulence generator—20%; for the PP-7 one—13%; in all other cases—5%.

Table 1
Parameters c and m entering the dependence (6)

Turbulence generator	Number of holes	c	m
S-1	—	0.38	0.21
PP-25	25	11.1	0.15
PP-13	13	16.6	0.12
PP-7	7	20.2	0.11

Degeneration of velocity fluctuations behind the turbulence generators is illustrated by Fig. 3. As was shown in [17, 20, 21], for the above turbulence generators the dying down of pulsations corresponds to the following decey law of uniform turbulence behind grid [24].

$$\frac{1}{Tu^2} = c\left(\frac{x'}{M} + \frac{x'_1}{M}\right)^m, \tag{7}$$

provided that the diameter of the turbulence generator's hole is taken as the characteristic scale M. Here c and m and constants, x'_1 is the coordinate of virtual origin, the origin of the x'-axis corresponding to the point where the turbulence generator is installed. As was found experimentally, the power exponent m equalled 1.1–1.6, which corresponds to the initial turbulence degeneration step (see tabulated data in [21]).

One of the most important flow characteristics is the

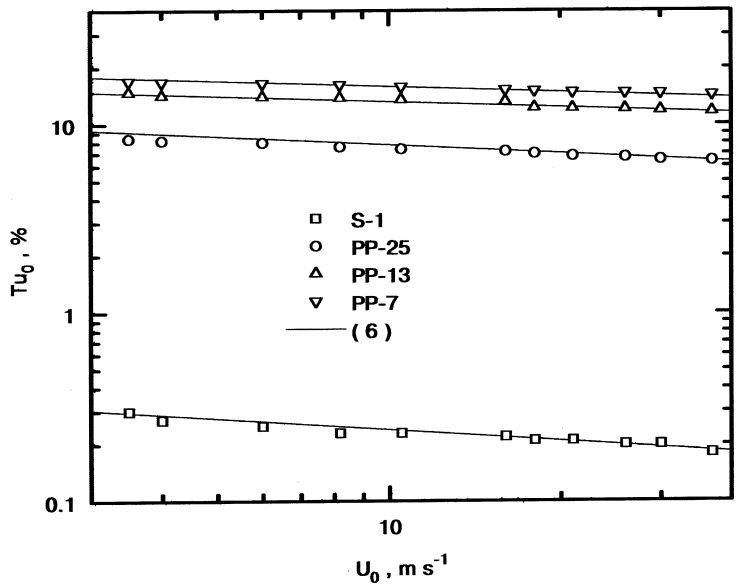

Fig. 2. Turbulence level in the stream behind different turbulence generators.

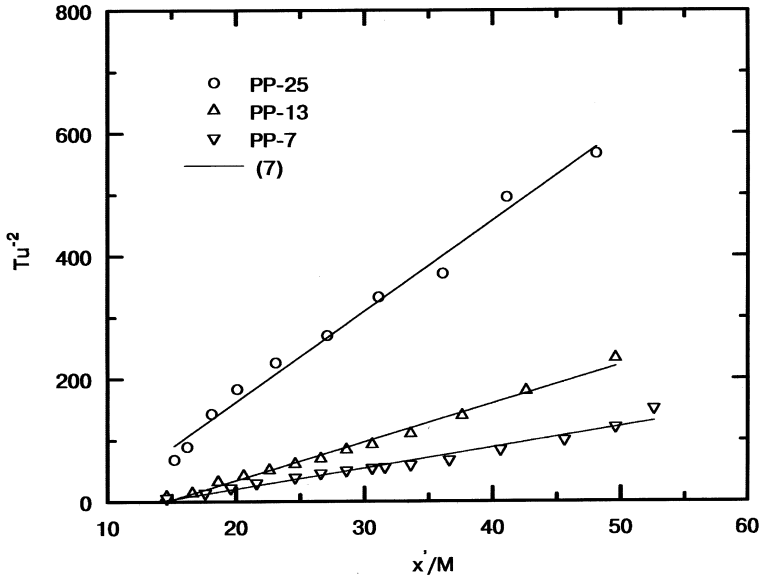

Fig. 3. Turbulence degeneration along the cylindrical channel.

energy spectrum of velocity fluctuations. The values of power spectrum for the longitudinal component of pulsating velocity $E_u(f)$ at the channel axis are shown in Fig. 4. As seen from the figure, there are three regions in the spectrum: the low-frequency one, the one where 'the Kolmogrov law of $-5/3$' is valid [23]:

$$E_u(k) = c_u \varepsilon^{2/3} k^{-5/3}, \quad (8)$$

and the high-frequency region. The extention of the stationary value $E_u(f)$ in the low-frequency region turned out to be highest for the stream behind the S-1 net, and it amounted to more than two orders of magnitude. Upon increasing the initial turbulence, the low-frequency region contracted with simultaneously increasing power of pulsations over the whole spectral range and, especially, in its low-frequency region. The interval where the 'law of $-5/3$' holds at the lowest turbulence $Tu_0 = 0.2\%$ is less than one decade, while at the highest turbulence

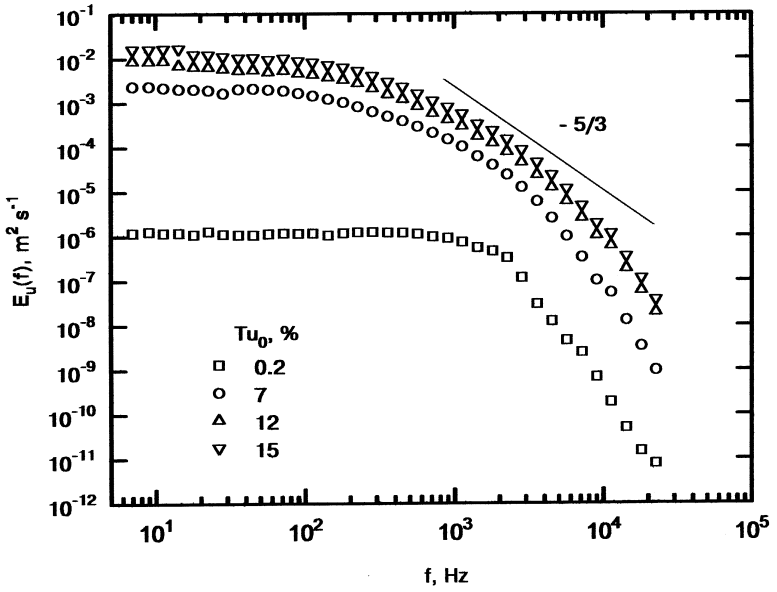

Fig. 4. Spectrum of longitudinal velocity pulsations at the inlet of the working section.

$Tu_0 = 15\%$ explored it extends over the range of one and a half order of magnitude. No discrete outshoots in the measured spectrum of turbulence energy was found. The integral longitudinal turbulence scale l_u was determined from the power spectra using the Taylor hypothesis [23]. The value of the macro-scale at the inlet of the working section is determined by characteristic dimensions of turbulence generator used (i.e., by diameter of its holes and by separation between them) as well as by the contraction ratio of the converging tube. At $Tu_0 = 7$–15%, $U_0 = 7$–15 m s^{-1} and $l_u = 8$–12 mm, the macroscale was 6 mm for the S-1 net.

The velocity profiles across the boundary layer at the jet injection section are shown in Fig. 5. In the same figure, the theoretical dependence for the velocity profile in the power forms (4) for two values of power exponent $1/n = 1/7$ ($A(n) = 0.717$) and $1/n = 1/12$ ($A(n) = 0.797$) is presented. As seen from Fig. 5, the measured velocity profiles across the boundary layer compare well with the velocity profile in the power form (4): in the low-turbulent stream ($Tu_0 = 0.2\%$) the power exponent $1/n = 1/7$, while in the high-turbulent stream the exponent increases (in line with the data reported in [17, 18]) and at $Tu_0 = 15\%$ $1/n = 1/12$.

Using properly treated data by different authors, in [20, 21] an empirical linear dependence of the exponent n in the power velocity profile (4) upon Tu_0 has been proposed:

$$n = n_0 + cTu_0 \tag{9}$$

with the coefficients $n_0 = 5.5$ and $c = 0.43$ (the dimensionality of Tu_0 here is %).

The measured velocity profiles are represented in generalized coordinates as $\varphi = f(\eta)$ in Fig. 6. In the same figure, the linear law

$$\varphi = \eta \tag{10}$$

and the law of wall

$$\varphi = \frac{1}{k}\ln\eta + C \tag{11}$$

are shown by lines, where the turbulence constants are: $k = 0.41$ and $C = 5.0$. As seen from the figure, the measured velocity profiles agree well with the two-layer scheme of near-wall turbulence: below $\eta \approx 11.5$—viscous sublayer, at $\eta > 11.5$—turbulent core—the region where 'the logarithmic law of wall' (11) holds. In the outer region of the boundary layer, the track 'law of wake' is normally used [17, 23]:

$$\varphi = \frac{1}{k}\ln\eta + C + \frac{\Pi}{k} f\left(\frac{y}{\delta}\right), \tag{12}$$

where $f(y/\delta)$ is the wake function. In this work, the wake function is the Coles–Hinzeform

$$f\left(\frac{y}{\delta}\right) = 1 - \cos\left(\pi\frac{y}{\delta}\right) \tag{13}$$

was adopted. The measured velocity profiles agreed well with the linear dependence (10) in the viscous-sublayer region, with the law of wall (12) in the turbulent-core one and with the track law (12) with the wake function (13) in the outer region of boundary layer. The parameter Π entering equation (12) varied from the value $\Pi = 0.55$ (the displacement thickness $\delta^* = 0.37$ mm) for the low-

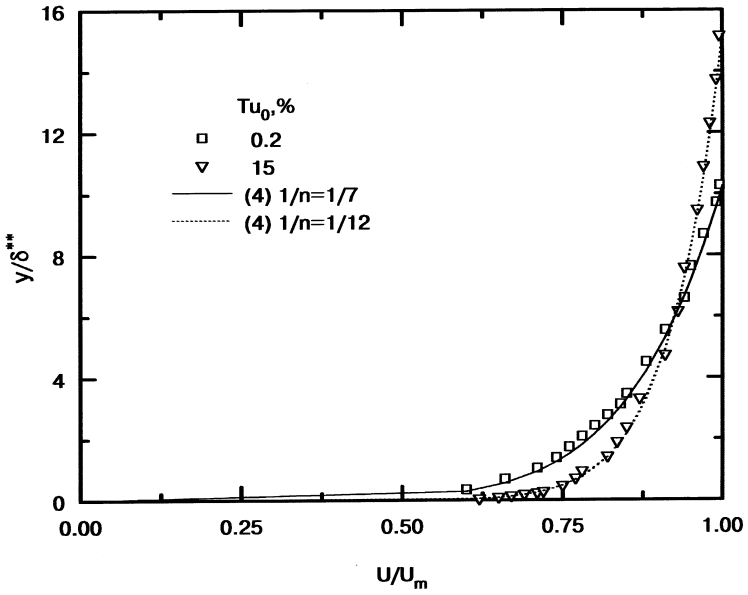

Fig. 5. Velocity profile across the boundary layer of stream.

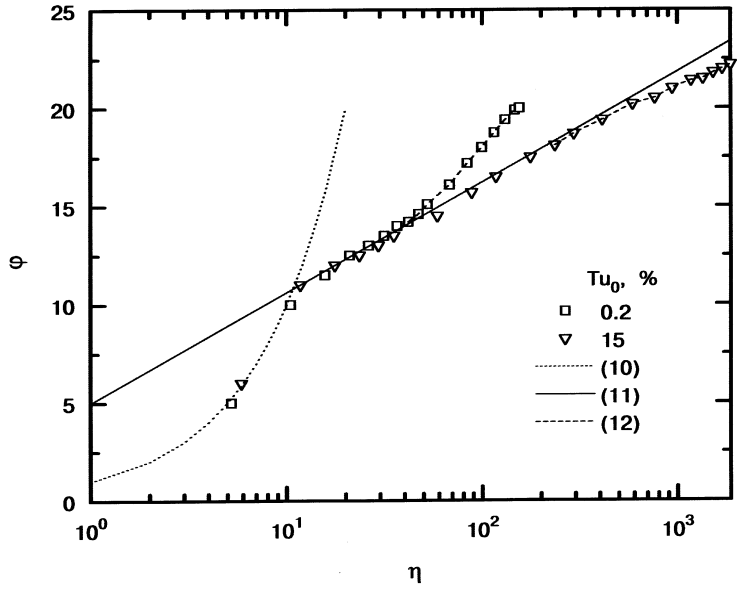

Fig. 6. Velocity profile across the boundary layer of stream in universal coordinates.

turbulent flow ($Tu_0 = 0.2\%$) down to the negative value $\Pi = -0.25$ at the turbulence level $Tu_0 = 15\%$ ($\delta^* = 2.46$ mm), which is in accord with experimental data [17, 18].

The distribution of the longitudal component of pulsational velocity across the boundary layer is presented in [21]. The profile of pulsations at different turbulence levels corresponds to a typical distribution characteristic of the developed near-wall turbulent flow: a weak increase of pulsations in the outer region of the boundary layer and a near-wall maximum which is situated in the buffer region at the boundary between the viscous sublayer and the turbulent core. At increasing turbulence level, the level of pulsations raises both in the outer region and in the near-wall one. For example, in the low-turbulent stream ($Tu_0 = 0.2\%$) the maximum value is 12.5%, while in the high-turbulent one ($Tu_0 = 15\%$) 17.6%. As experiments with the PP-4 turbulence generator (4 holes) have shown, the standard distribution with the maximum of pulsations situated near wall breaks down at $Tu_0 = 20\%$, when a monotonic growth of fluctuations upon passing from wall to outer border of boundary layer is observed.

To organize the film cooling, the coolant was fed through a tangential annular slot. The measurements have shown that the velocity profile inside slot at the injection parameter $m > 0.2$ is close to the parabolic one. The thickness of boundary layer in the slot roughly equals a half of the slot height, while the turbulence level in the jet core amounts to 4–5% at small injection parameters ($m < 1$) and to 5–6% at higher injection parameters ($m > 1$) when $Re_s = 2000$–4500.

The behaviour of the turbulence degeneration along the channel axis at blowing the coolant is presented in [20, 21]. A considerable decreasing of the pulsational velocity behind turbulence generators takes place in front of the slot exit. Downstream along the channel, the value of Tu decreases more weakly: for example, for the PP-7 turbulence generator, the turbulence level decreases from 15% down to 9%, while for the S-1 net from 0.2% down to 0.19%. The gas injection exerts practically no effect on the turbulence degeneration at the channel axis.

3. Experimental results and discussion

The problem on the thermal mixing of a wall jet with a cocurrent stream is usually considered for two types of wall boundary conditions: an adiabatic surface ($q_w = 0$) and a surface with a thermal flux ($q_w \neq 0$). In order to experimentally determine the local heat-transfer coefficient at injection of gas into boundary layer using expression (1), one should know the wall temperature under adiabatic conditions.

In [20, 21, 24], it has been established that the intensity of external-flow turbulence exerts a substantial influence on the adiabatic surface temperature during the development of wall jets in channels. The action of external turbulence on the mixing process of a wall jet with a main stream can be quantitatively characterized by the injection parameter m [21]. Experimental data on the film cooling effectiveness Θ, the parameter commonly used for solving thermophysical problems on the adiabatic surface, are presented in Fig. 7. The film cooling effectiveness in the low-turbulent flow is seen to attain its

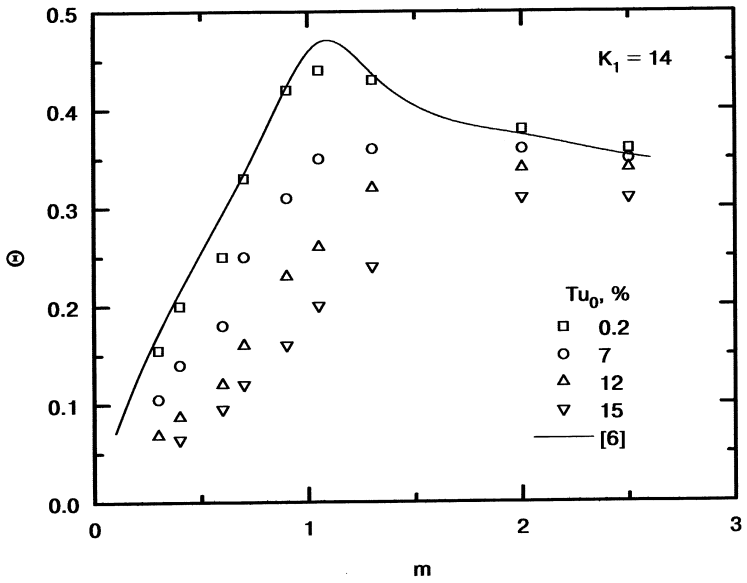

Fig. 7. Effect of injection parameter on screen effectiveness.

highest at $m \approx 1$. The line at the same figure shows the calculated dependence for the low-turbulent stream at $K_1 = 14$ [6]. The experimental results at $Tu_0 = 0.2\%$ are seen to satisfactorily agree with the calculation results [6]. The increased external turbulence worsens the heat-shielding properties of the film cooling over a wide range of m_1 (as compared to data for $Tu_0 = 0.2\%$). The behaviour of the screen in the high-turbulent flow is qualitatively different: the film cooling effectiveness grows monotonically with increasing m. As contrasted to the low-turbulent flow, the effectiveness of the high-turbulent screen keeps on growing as well at $m > 1$, approaching asymptotically the Θ value for $Tu_0 = 0.2\%$. From $m =$ 2–2.5, the film cooling effectiveness for the turbulized external flow becomes practically independent of the velocity of the injected gas. Therefore, further increase in the mass-flow rate of the coolant does not change substantially the protective properties of screen, and, consequently, such regimes are not economical of energy.

Such a substantial influence of the injection parameter m and of the turbulence level of stream Tu_0 on the effectiveness of film cooling on the adiabatic wall ($q_w = 0$) suggests that, when a wall heat flux is present ($q_w \neq 0$), approximately the same effect of the parameters m and Tu_0 on the heat-transfer coefficient would be observable. However, in the problem with heat transfer, the effect due to stream turbulence upon α can be allowed for through assuming the adiabatic wall temperature T_{wa} in equation (1) to be dependent upon Tu_0. In this case both in the low-turbulent stream and in the high-turbulent one, heat transfer can be calculated according to equation (5) provided that the Stanton and Reynolds numbers St and Re_T^{**} are determined with due regard for the adiabatic wall temperature T_{wa}.

At the first stage of the study of the effect of free-stream turbulence intensity on the wall jet heat transfer, the data were treated with no regard for T_{wa}. The corresponding results are shown in Fig. 8. In the experiments, the heat-transfer coefficient

$$\alpha = \frac{q_w}{T_w - T_0} \tag{14}$$

and, correspondingly, the Stanton number were determined from the difference between the wall temperature and the stream one, while the Reynolds number Re_T^{**} was determined from the integral energy conservation law:

$$Re_T^{**} = \frac{\alpha x}{\mu_0 c_{p0}}. \tag{15}$$

As is seen from the figure, in this treatment of data the increase in turbulence from 0.2% up to 20% results in a growth of the heat-transfer coefficient by a factor of 1.5–2. Under low-turbulent conditions, the correlation $St = f(Re_T^{**})$ disagrees with the power heat-transfer law. This is connected with that the Stanton number in the experiments is determined with no regard for the adiabatic wall temperature T_{wa}.

The effect of the turbulence level of stream on the heat-transfer coefficient determined according to (1) using the adiabatic wall temperature for three values of the injection parameter is shown in Fig. 9. The experiments were carried out in two steps. First, the wall jet of temperature T_s was injected into the stream of temperature T_0 at a

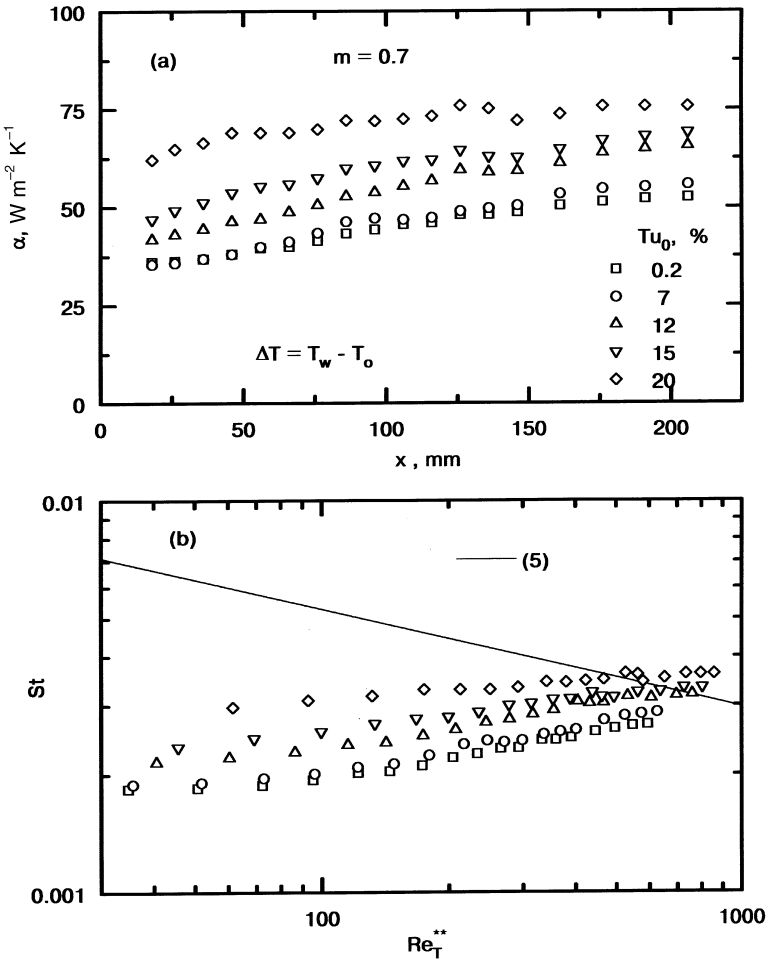

Fig. 8. Heat transfer in the screen region ($\Delta T = T_w - T_0$).

fixed m, and the temperature T_{wa} of the adiabatic wall of the cylindrical channel was measured. Then the channel was heated up in the regime $q_w = \text{const}$ and the wall temperature T_w was determined. The cooling effectiveness Θ evaluated from T_{wa} was found to agree with the experimental data obtained for a cylindrical channel with thermally isolated walls [21].

It follows from Fig. 9 that flow turbulization increases the heat-transfer coefficient by 20–30% only at $m < 1$, the effect at $m = 0$ exceeding that at $m = 0.7$. In the case when the velocity of jet exceeds that of stream ($m = 2$), the heat-transfer coefficient is practically independent of stream turbulence intensity. The latter provides an evidence that the wall jet acts like a buffer impeding the penetration of turbulent vortices generated by the main stream.

In Fig. 10, the experimental data shown in Fig. 9 for $m < 1$ are represented as $St = f(Re_T^{**})$ dependences. In the experiments, the Stanton and Reynolds number were determined with taking into account the adiabatic wall temperature according to (2) and (15). The line shows the power heat-transfer law (5) for the 'standard' boundary layer. As is seen from Fig. 10(a), the heat transfer data for conditions with no gas injection ($m = 0$, $T_{wa} = T_0$) for different Tu_0 do not coincide. For the low-turbulent stream, the experimental dots agree well with the calculated straight line (5). Deviation of the experimental data from (5) at $Re_T^{**} < 250$ is due to the effect of flow pre-history. At increasing turbulence level, the Stanton numbers fall above the theoretical dependence.

The similar effect is also exerted on heat transfer by the turbulization of flow during the injection of coolant ($m = 0.7$) (Fig. 10(b)) in the case when the Stanton and Reynolds numbers are determined using the adiabatic wall temperature according to (2). The experimental data for the low-turbulent stream ($Tu_0 = 0.2\%$) treated in this manner fit the power dependence (5) for heat transfer. As is seen from Fig. 10(b), for the high-turbulent stream,

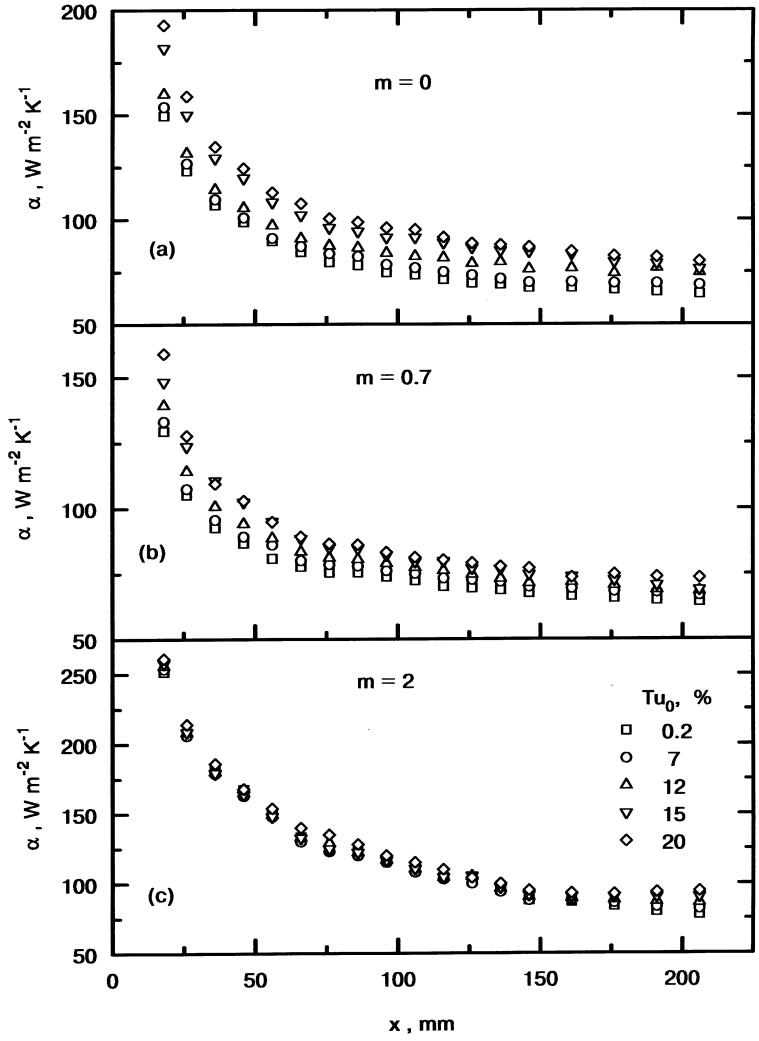

Fig. 9. Heat-transfer coefficient in the screen region ($\Delta T = T_w - T_{wa}$).

the account of the wall temperature turns out to be insufficient to generalize data, and the relative heat-transfer function ψ should be used like in the case when it is introduced to take account of the effect of external turbulence at the plate without injection [3].

The influence of the external turbulence on the relative heat-transfer function $\psi = (St/St_0)$ at $Re_T^{**} = \text{idem}$ for two regimes is illustrated by Fig. 11. In the experiments, St_0 is the Stanton number at the turbulence level 0.2%. As seen from the figure, the growth of the turbulence intensity up to 20% results in the ψ value increased by 26% and 20% at $m = 0$ and 0.7, respectively. In the zone where the initial conditions exert no effect, the relative heat-transfer function is independent of Re_T^{**}. Hence, the relative heat-transfer law at the action of external turbulence can be approximated by the following linear dependence [20, 21]:

$$\psi_{Tu} = \left(\frac{St}{St_0}\right)_{Re_T^{**}} = 1 + cTu_0 \tag{16}$$

with the coefficient $c = 0.013$ at $m = 0$ and $c = 0.01$ at $0 < m < 1$.

The jet laws [3, 6] are known to govern the film cooling in low-turbulent streams at high injection parameters ($m > 1$). The effect of increased turbulence on heat transfer in this case is illustrated by Fig. 12, where the Stanton number of the secondary stream is determined according to (2):

$$St_s = \frac{q_w}{\rho_s c_{ps} U_s (T_w - T_{wa})}. \tag{17}$$

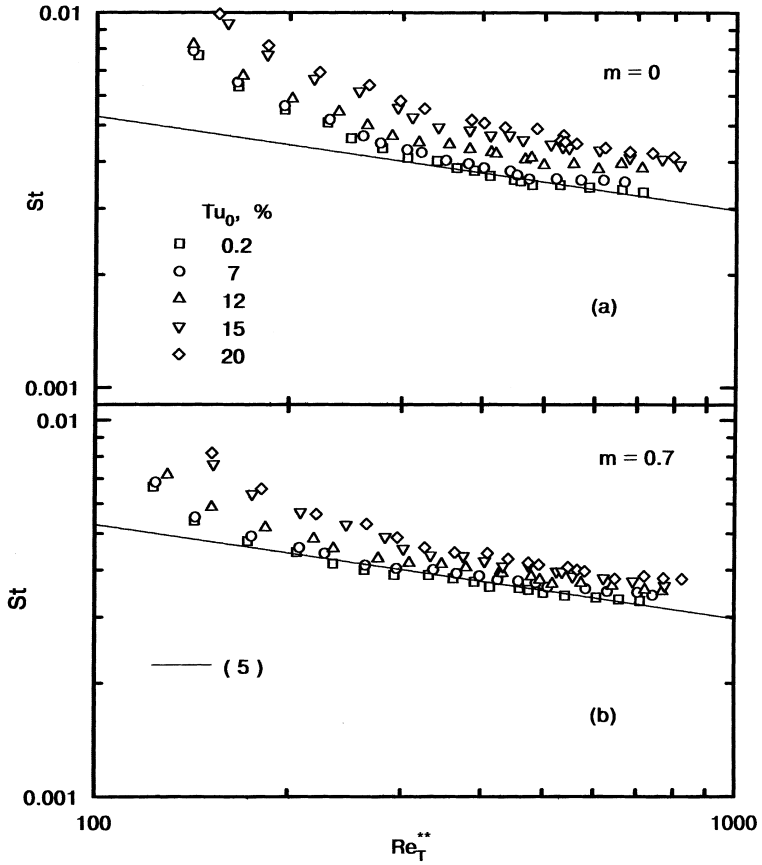

Fig. 10. Heat transfer in the screen region ($m < 1$).

The line shows the heat-transfer law for the wall jet [3].

$$St_s = \frac{0.12}{Re_S^{0.2}(x/s \cdot Pr)^{0.6}} \tag{18}$$

As is seen from the figure, in this treatment of data, the turbulence intensity exerts no effect on the heat-transfer law in the wall jet. Thus, at the injection parameters $m > 0$, the heat-transfer calculations for high-turbulent streams can be carried out using dependence (18) being characteristic of low-turbulent jet flows.

The effect of external turbulence on heat transfer in a near-wall cocurrent jet is determined by m. The experimental data illustrating this fact are presented in Fig. 13. Here St_h and St_l are the Stanton numbers at high and low ($Tu_0 = 0.2\%$) turbulence level of stream. As is seen from the figure, the effect due to turbulence level on the relative heat-transfer function is noticeable at $m < 1$ and insignificant at $m > 1$. The obtained result is consistent with those on the effectiveness (see Fig. 7), where the effect of high turbulence also becomes less pronounced at $m > 1$. In this case, the energy of turbulent vortices of the external stream is essentially smaller than the kinetic energy of the wall jet. The wall boundary layer exhibits considerable stability to external stream disturbances, and heat transfer is determined by jet laws.

4. Conclusions

The action of the cocurrent-stream turbulence on the thermal mixing with a wall jet depends upon the injection parameter m, i.e., on the proportion between the specific momenta of jet and stream. At $m < 1$, the maximum effect due to turbulence is observable, while at $m > 1$ the effect due to turbulence is insignificant.

In the case when the momentum of jet is smaller than that of stream ($m < 1$), the effect due to turbulence depends on the wall boundary conditions. In the problem on the adiabatic wall, Tu_0 exerts a considerable influence on the mixing layer, and, as a result, the dimensionless wall temperature may change more than two-fold. When calculating the cooling effectiveness, the effect due to Tu_0 can be taken into account by varying the starting heated length of wall jet and deforming both the velocity profile and the relative heat-transfer function (16) [21–22]. For

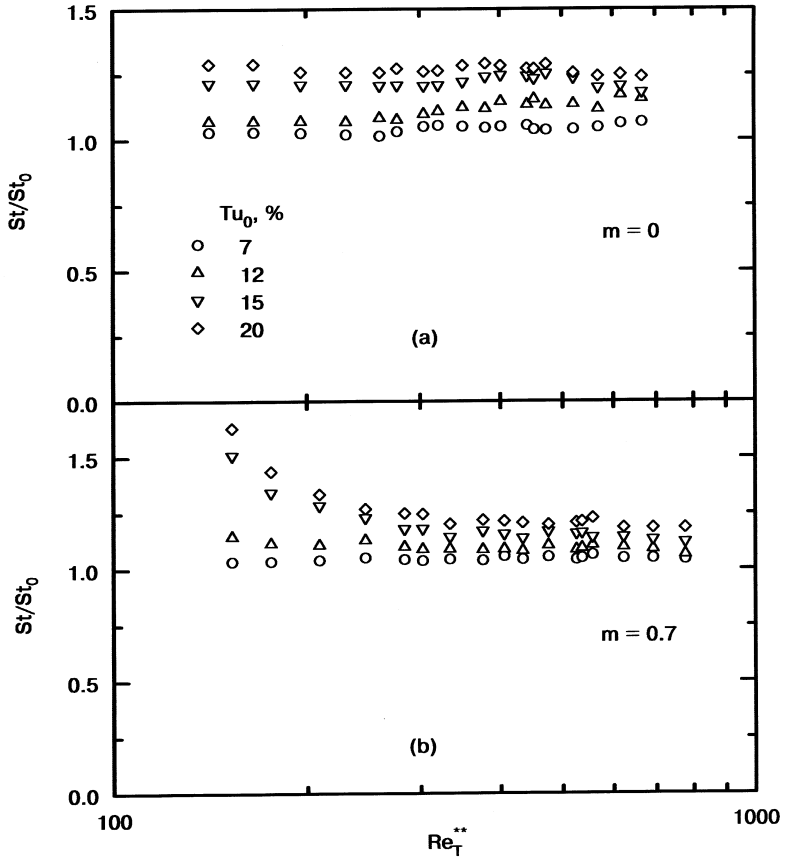

Fig. 11. Effect of flow turbulence on relative heat-transfer function ($m < 1$).

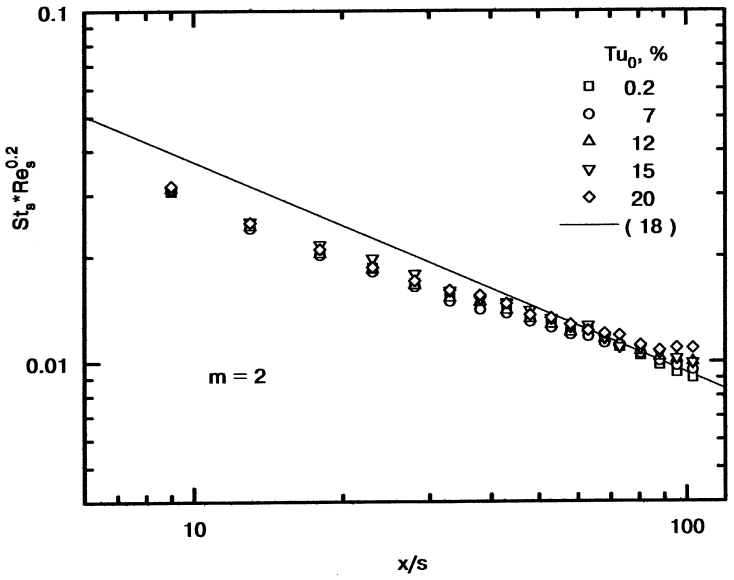

Fig. 12. Effect of turbulence on heat transfer in the wall jet ($m > 1$).

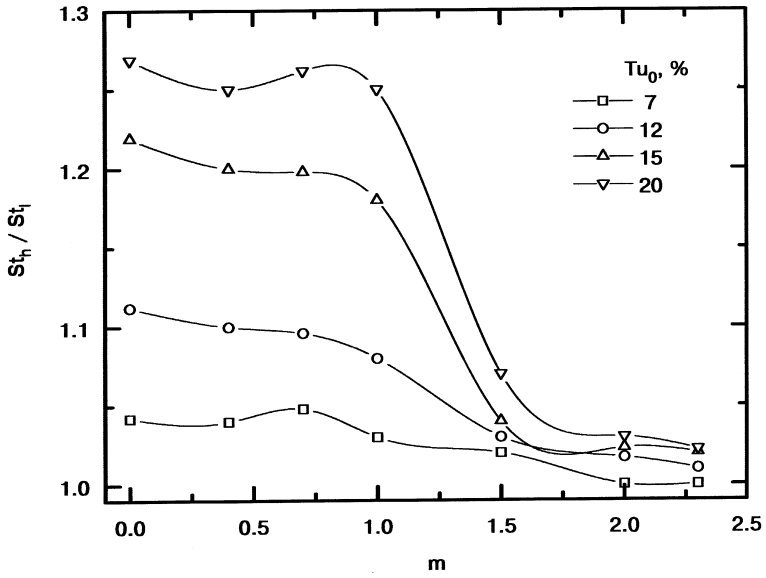

Fig. 13. Effect of injection parameter on relative heat-transfer function.

the wall with a heat flux, the wall heat transfer is more stable with respect to Tu_0, and its variation does not exceed 20–30%. In this case, the effect due to turbulence can be allowed for through the adiabatic wall temperature in the heat-transfer law for near-wall processes (5) and through the relative heat-transfer function in the form (16).

At high injection parameters ($m > 1$), the effect of turbulence on the thermal mixing is insignificant for both the thermally insulated and the heat-conducting walls. Therefore, both the cooling effectiveness and the heat-transfer coefficient should be calculated according to dependences characteristic of near-wall jet flows.

Application of heat-transfer law in the power form (3) and of the relative heat-transfer function for the near-wall turbulence allows to take account of the joint action of several factors, e.g., a longitudinal pressure gradient, non-isothermility or compressibility [3]. At $m < 1$, when the near-wall turbulence generalities prevail, the use of the relative function (16) permits an estimation of heat transfer to be made for a wider range of turbulent flows (e.g., for the supersonic high-turbulent stream).

Turbulence is known to be characterized by several parameters, the main of which are turbulence intensity and integral scale. From this standpoint, additional studies of the effect of the initial integral turbulence scale on the heat transfer in wall jet is required.

Acknowledgements

The authors are indebted to S. Ya. Misyura for his assistance in carrying out experiments. The work was supported by the Russian Foundation for Basic Research (grant N 98–02–17898a).

References

[1] E.R.G. Eckert, R.M Drake, Heat and Mass Transfer, McGraw-Hill, New York, 1959.
[2] S.S. Kutateladze (Ed.), Heat Transfer, Mass Transfer and Friction in Turbulent Boundary Layer, SO AN USSR, Novosibirsk, 1964.
[3] S.S. Kutateladze, A.I. Leont'ev, Heat Transfer, Mass Transfer and Friction in Turbulent Boundary Layer, Hemisphere, New York, 1990.
[4] V.P. Lebedev, Experimental investigation of turbulent boundary layer on a flat plate at step distribution of heat flux, J. Appl. Mech. Tech. Phys. 4 (1969) 112–115.
[5] R.J. Goldstein, Film cooling, Advances in Heat Transfer 7 (1971) 321–379.
[6] E.P. Volchkov, Wall Gas Film Cooling, Neaka, Novosibirsk, 1983.
[7] T. Cabeci, P. Bradshaw, Physical and Computation Aspects of Convective Heat Transfer, Springer, New York, 1984.
[8] A.I. Leont'ev et al. (Eds.), Thermal Protection of Plasma Generator Walls, Institute of Thermophys, Novosibirsk, SB RAS, 1995.
[9] S.C. Kacker, J.H. Whitelaw, The effect of slot height and of slot turbulence intensity on the effectiveness of the uniform density, two-dimensional wall jet, Trans. ASME J. Heat Transfer, 90 (1968) 469–484.
[10] G.I. Sadovnikov, B.M. Smol'sky, V.K. Shchitnikov, Heat transfer on a flat place in near-wall jet with different initial turbulent levels, in: Studying of Heat-Transfer Processing

in Complex Systems, ITMO of the Buelorussian Acad. Sci., Minsk, 1974, pp. 81–91.
[11] G.J. Sturgess, Account of film turbulence for predicting film cooling effectiveness in gas turbine combustors, Trans. ASME, J. Engin. Power, 102 (1980) 524–534.
[12] V.I. Kosenkov, Plane turbulent semi-restricted jet on a permeable surface, Izv. SO AN SSSR, Ser. Tekhn. Nauk, 1 (1989) 23–28.
[13] V.V. Glazkov, M.D. Guseva, B.A. Zhestkov, V.P. Lukash, On initial turbulence effect on permeable wall cooling effectiveness, Engng. Phys. 36 (1979) 965–971.
[14] D.B. Spalding, Boundary-layer theory applied to film-cooling processes. Progress Heat Mass Transfer 4 (1971) 279–296.
[15] J.C. Simonich, P. Bradshaw, Effect of free-stream turbulence on heat transfer through a turbulent boundary layer, Trans. ASME J. Heat Transfer 100 (1978) 671–677.
[16] M.F. Blair, Influence of free-stream turbulence on turbulent boundary layer heat transfer and mean profile development, Trans. ASME J. Heat Transfer 105 (1983) 33–47.
[17] E.P. Dyban, E. Ya. Epick, Heat Mass Transfer and Hydrodynamics of Turbulized Flows, Naukova Dumka, Kiev, 1985.
[18] A. Pyadishyus, A. Shlanchyauskas, Turbulent Heat Transfer in Wall Layers, Mokslas, Vilnyus, 1987.
[19] B.P. Mironov, V.N. Vasechkin, N.I. Yarygina, V.N. Mamonov, Heat and mass transfer at high free-stream turbulence as a function of injection rate, Heat Transfer—Soviet Research 13 (5) (1981) 54–65.
[20] V.P. Lebedev, V.V. Lemanov, S. Ya. Misyura, V.I. Terekhov, Effects of turbulence intensity on slot protection performance, J. Appl. Mech. Tech. Phys. 32 (1991) 360–364.
[21] V.P. Lebedev, V.V. Lemanov, S. Ya. Misyura, V.I. Terekhov, Effects of flow turbulence on film cooling efficiency, International Journal of Heat and Mass Transfer 38 (1995) 2117–2125.
[22] V.V. Lemanov, S.Ya. Misyura, Measurements in a two-dimensional turbulent flow by means of an automated hot-wire anemometer, Izv. SO AN SSSR, Sib. Phys. Tech. J. 3 (1991) 112–115.
[23] A.S. Monin, A.M. Yaglom, Statistical Field Mechanics, vol. 2, MIT Press, Cambridge, 1975.
[24] L.W. Carlson, E. Talmor, Gaseous film cooling at various degrees of hot-gas acceleration and turbulence levels, International Journal of Heat and Mass Transfer 11 (1968) 1695–1713.